

The X-ray Point Source Population of the Omega Nebula

Getman K.V., Feigelson E.D., Townsley L.K., Garmire G.P., Broos P.S. (Penn State), & Tsuboi Y. (Chuo University)

ABSTRACT

We have obtained a 40 ks X-ray image of the high-mass star forming region of M17 (the Omega Nebula) with the ACIS-I detector on board the Chandra X-Ray Observatory. In addition to a prominent soft diffuse X-ray emission our image with a sensitivity limit of $\log L_x \sim 29.7$ erg/s revealed 889 X-ray sources. While 832 of these sources can be identified with cluster members and foreground stars known from JHK band surveys, more than the half of 57 unidentified objects are most likely new cluster members. The X-ray luminosity function of the detected young stars spans a range of $\log L_x \sim 29.7\text{--}33.5$ erg/s in the 0.5–8 keV band, and absorption ranges from $\log N_H \sim 21.7\text{--}23.5$ cm $^{-2}$. The X-ray lightcurves of several sources reveal powerful flares with parameters typical for X-ray active young stellar objects. We construct and analyze the X-ray spectra of the stronger sources and derive plasma temperatures between 0.7 keV and 5 keV for the T Tauri stars and deeply embedded young stellar objects in M17, and higher temperatures up to 12 keV for many flaring sources. We find that most of the deeply embedded X-ray YSOs are distributed in or southwest of the ionization front excited by the central OB cluster. This distribution supports the theory of induced star formation in the molecular cloud, most actively in the southern bar. We describe in detail the X-ray properties of the most interesting individual sources, including KW object, ultra compact HII region M17-UC1, and the protostellar object 182022.9-161152 deeply embedded within the dense molecular core.

INTRODUCTION

The Omega Nebula (M17), one of the most luminous HII regions in the Galaxy, is situated at the edge of a massive and dense molecular cloud at a distance of 1.6 kpc from the Sun. Its major morphological components [see Figure 1] are: 1. the photoionized nebular seen as Northern and Southern emission bars in the IR and radio bands [e.g. 5]; 2. the central cluster of dozens of O- and early B-type stars, which excites the nebular, identified by optical and near-IR spectroscopy [e.g. 7]; 3. the dense cold molecular material surrounding the two bars [14] with active star formation, including new rich stellar clusters [11]. Observations of M17 play a significant role in helping astronomers to better understand the conditions in giant molecular clouds and in photodissociation regions and the propagation of star formation. Optical and near-IR studies could detect only a modest fraction of the M17 stars because of the high stellar concentration and the large line-of-sight extinction. The Chandra spatial resolving power and great sensitivity gives us ability to find many more new members of star clusters in M17 and to improve the census of the star cluster membership. The discovery of the soft diffuse X-ray emission by Chandra in M17, most likely arising from the fast O-star winds, has been reported already in [18]. The present work focuses on the study of the X-ray properties and the spatial distribution of numerous point sources detected in the region. We confirm the findings of the latest deep near-IR survey [11]: most of the protostellar candidates are distributed in and near the ionization front excited by the central OB cluster, giving the evidence of induced star formation in the nebular (bar) regions. We report the discovery of dozens of new protostellar objects, previously unknown. In addition our data indicate the ongoing star formation process in the northern cloud core (not covered by deep near-IR survey) which is independent of the star formation in the nebular region.

OBSERVATION AND DATA REDUCTION

Chandra observed M17 on March 2-3 2002 for 39.4 ks as a part of the guaranteed time observer program using the ACIS-I imaging array [6] with the field of view (FOV) of about $17' \times 17'$. The aimpoint was chosen to place the heavily obscured O4V-O4V binary of the OB cluster at the center of the image, so that 3 major morphological components were included in the FOV. Our custom processing, starting with the Level 1 data stream, is described in detail in [18]. For the source detection we employed the routine "wavdetect", using the default "Mexican Hat" wavelet with the significance threshold of 10-6. To enhance selection sensitivity we ran "wavdetect" separately for a series of three 1024x1024 pixel concentric images at different pixel resolutions for each of the three (soft, hard, full) energy bands. Upon visual inspection of the image, 10 sources appeared to be spurious and a few dozens of new sources were added to the source catalog. The merged catalog produced 889 sources. We applied the "acis_extract" routine from the Tools for X-ray Analysis [10] in order to: 1. extract event lists for each source, using the polygonal region generally chosen to match the contour of 90% encircled energy from the PSF (the smallest apertures were chosen for crowded sources) at the fiducial energy of 1.5 keV; 2. extract the background from the squeeze-cheese event list and to scale it, using the integrated exposure in the region; 3. compute instrumental responses (RMF and ARF) with ARFs, corrected for the PSF fraction enclosed by the extraction regions and for the hydrocarbon build-up on the detectors [9]; 4. create source spectra and scaled local background spectra; 5. group spectra; 6. compute photometry; and 7. perform automated spectral fitting spanning the XSPEC v11.2 tool.

SPECTRAL AND TIMING ANALYSIS

For all sources containing at least 60 counts we performed a spectral analysis, with the aim to derive the plasma temperatures and to determine the X-ray luminosities. We used the XSPEC model "mekal", describing the emission from the optically thin thermal plasma and used "wabs" for the absorption model. Although the coronae of active stars are not non-thermal, given the rather low number of the detected X-ray photons, we tried to fit most of the spectra with a single-temperature model to characterize the coronal temperature distribution by a single "characteristic" temperature (as it has been done in many past works on star formation regions). In Figure [2] we show the plasma energies plotted versus the extinction corrected [0.5-8] keV band X-ray luminosities. Many stars have plasma energies between 0.7 and 3 keV, which is a typical range of X-ray active T-Tauri stars [e.g. 4], although there are even more sources with the energies rather high up to 10 keV; many of them showed X-ray flares during the observation [similar results find e.g. 16]. Figure [3] shows several examples of representative X-ray spectra for different types of X-ray sources in M17 region.

Due to the presence of the diffuse interstellar medium between the Sun and M17 all members of the region suffer a visual extinction of $A_V > 3$ mag ($n_H > 6 \times 10^{21}$ cm $^{-2}$) and most of the detected members additionally suffer a high local extinction, as the result, spectra of M17 members are moderately or highly absorbed. The three top panels represent spectra of flaring T-Tauri stars with temperatures higher than 3 keV. The next four panels represent spectra of early OB stars with the unusually high temperatures (much hotter than current stellar wind models predict, find similar results in e.g [17]) for O4V-O4V binary, located in the center of OB cluster (at the aimpoint of our image). The last two panels show spectra of protostellar candidates deeply embedded in a molecular cloud.

In Figure [4] we present the lightcurves of 18 sources that are exhibiting significant systematic variability. Some of them show a typical profile with rise and decay times of a few hours, resembling the classical impulse flares of the Sun, while the others show interesting features: the peak in the hard-band lightcurve occurs about one hour earlier than the peak in the soft-band lightcurve; only soft-band lightcurve shows a significant increase during the flare; rapid increase of the count rate without a following significant decay; periodic variability, e.g. rotational variability.

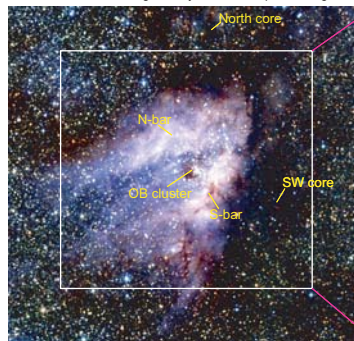


Fig. 1. - JHK image of the Omega Nebula (roughly $23' \times 25'$) from the 2MASS survey showing the central OB cluster and ionized gas surrounded by the dark molecular cloud. The white box indicates the ACIS-I FOV.

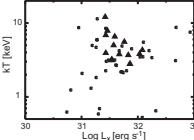


Fig. 2. - Plasma energy versus X-ray luminosity as determined in the spectral fits for the strongest X-ray sources. No correlation is seen. Flaring sources, marked by triangles, have energies higher than average.

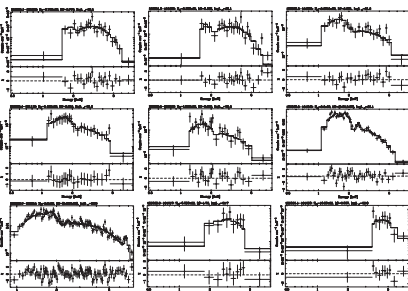


Fig. 3. - Some representative ACIS spectra of X-ray sources in M17. In the top panels of each plot the points with error bars represent the grouped observed spectra; the continuous solid lines represent the best fit models. The residuals in units of contribution to chi-squared are plotted on the bottom panels.

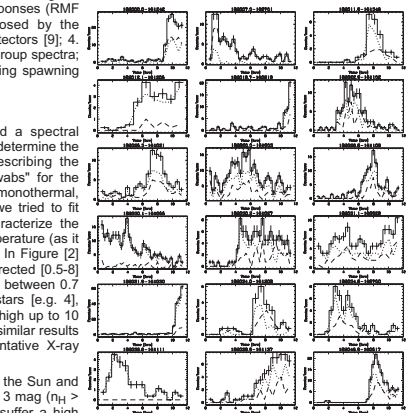


Fig. 4. - Lightcurves for the sources exhibiting strong variability during our Chandra observation. The histograms show the full (0.5-8.0 keV) energy band lightcurves, binned by 10-30 bins. The dashed lines represent the lightcurves for the soft (0.5-2.0 keV) band, while the dotted line for the hard (2.0-8.0 keV) energy band. Lightcurves demonstrate a wide range of different morphologies.

REFERENCES

- Brandt, W.N. et al. 2001, *aj*, 122, 2810
- Chini, R. et al. 2000, *apj*, 527, L33
- Codella, C. et al. 1996, *apj*, 311, 971
- Feigelson, E.D. 1999, *arXiv preprint astro-ph/9903036*
- Felli, M. et al. 1998, *apj*, 496, L36
- Garmire, G.P. 2003, *procspice*, 4851, 28
- Hanson, M.M. et al. 1997, *apj*, 469, 699
- Hobson, M.P. et al. 1993, *mras*, 254, 1025
- http://www.astro.psu.edu/users/charles/xcontdir/xcont.html
- http://www.astro.psu.edu/xray/docs/TARA/ae_users_guide/
- Jiang, Z. et al. 2002, *apj*, 577, 245
- Johnson, C.O. et al. 1998, *apj*, 500, 302
- Klein, R. et al. 1999, *apj*, 513, L53
- Lada, C.J. 1976, *ajps*, 32, 603
- Nielbock, M. et al. 2001, *apj*, 537, 273
- Preibisch, T. et al. 2002, *aj*, 123, 1613
- Schulz, N.S. 2003, *Revista Mexicana de Astronomia y Astrofisica Conference Series*, 15, 220
- Townsley, L.K. et al. 2003, *apj*, 593, 874
- Tsuboi, Y. et al. 2001, *apj*, 554, 734
- Wang, Y. et al. 1993, *apj*, 419, 707

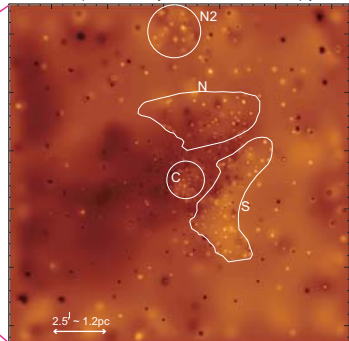


Fig. 5. - The ratio of the 2.0-8.0 keV (hard) to the 0.5-2.0 keV (soft) adaptively smoothed images. The bright sources are hard and the dark sources are soft. The polygons indicate the sampled regions (see text).

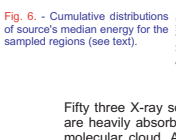


Fig. 6. - Cumulative distributions of source's median energy for the sampled regions (see text).

SPATIAL DISTRIBUTION OF X-RAY SOURCES

In Figure [5] we show the hardness ratio smoothed image of M17. It seems obvious that the spatial distribution of X-ray point sources of different energies resembles the location and shape of the major morphological components that have been known from previous radio, optical and IR observations. The X-ray S, and N regions include the edges of the molecular cloud and expanding ionization fronts, driven by the cluster members of the central OB cluster mainly by O4V-O4V binary, and seen as an S-bar and N-bar in radio band, or south and north ridges in mid-infrared [see Figure [7], 15]. The ionization fronts are advancing to the SW and North and sweeping up the diffuse ISM at the edges of the molecular cloud and compressing it. This could be the cause of density waves that progress through the cloud triggering gravitational instabilities and consequently fragmentation and the formation of new stars. The total number of X-ray stars exceeds 200 and 90 X-ray young objects within the S and N regions respectively. Under assumption of the similar intrinsic properties of the stars of the N and S regions, the source's median energy reflects the properties of the surrounding medium, and in this case the cumulative distribution for the source's median energy, shown in Figure [5], indicates that the S region suffers a slightly greater attenuation than the N region. The ISOCAM observations [13] presented the evidences of the on-going star formation in the northern part of M17, the cloud core M17-North, located $10'$ north of the Omega Nebula (out of our FOV). The spatial clustering of the young X-ray sources within the N2 region and cumulative distribution of source energy, distinctive from that of the N region, strongly suggest that the N2 region is a part of the M17-north complex.

Fig. 8. - The composite X-ray spectrum of 29 unidentified clustered sources located in S region.

Fifty three X-ray sources remain unidentified with any optical/IR object. They are heavily absorbed and must lie behind or be deeply embedded within the molecular cloud. As it is seen in Figure [7] the spatial distribution of these sources appeared to be non uniform with half of them clustered within the S region. Assuming the same nature of these 29 clustered sources, having a small number of counts, we combined them together to create a single composite spectrum [see Figure [8]]. For both models, "pow" and "mekal", their spectral fit results suggest that the amount of absorption, sources suffer, must be as large as $A_V \sim 25$ mag. For this extinction $A_V \sim 25$ mag, the X-ray flux limit of a faintest quasar with a photon of the central part of the index of 1.4 in a hard (2.0-8.0 keV) band in our ACIS Omega Nebula at 10.5 micron [15]. The sampled X-ray regions (polygons) resemble the shape and extragalactic source density is about 200-300 sources per square degree [1], or 1 in the field of S region, location of two mid-infrared ridges. Most of located within the part of the field where the molecular cloud has the average extinction greater than $A_V \sim 25$ circles, are clustered and in some parts the value might even exceed towards the S region. 40 mag, as suggested by CO and CS molecular line Green contours indicate the 1.3 cm continuum emissions from [20], we should consider most of them image of the Arc structure if not all to be deeply embedded into the molecular and M17-UC1 [12].

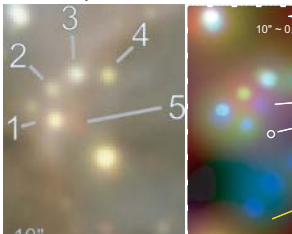
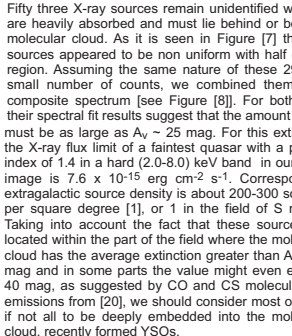


Fig. 9. - Enlarged view of the full-band raw Chandra image of the Arc area. Blue crosses indicate the location of H $_2$ O masers, while the black circle P3 sub-millimeter clump. 1.3 cm continuum emission is marked by green contours.

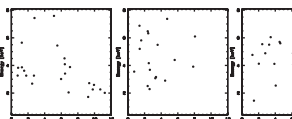


Fig. 10. - Enlarged view of the M17-UC1 area. (Left) Image from the deep near-IR survey [11]. (Right) Chandra "true-color" image.

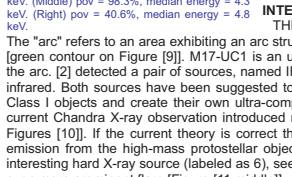


Fig. 11. - Photon arrival times and energies for the three detected embedded objects discussed in the text. (Left) $\text{pov}/\text{Poisson}$ probability for temporal variability = 85.7%, median energy = 3.3 keV. (Middle) $\text{pov} = 98.3\%$, median energy = 4.8 keV. (Right) $\text{pov} = 40.6\%$, median energy = 4.8 keV.

INTERESTING SOURCES

THE ARC (M17-UC1)

The "arc" refers to an area exhibiting an arc structure in the centimeter continuum map of the S bar [12] [green contour on Figure [9]]. M17-UC1 is an ultracompact HII region located near the center of curvature of the arc. [2] detected a pair of sources, named IRS 5N and IRS 5S, that exhibit the strong emission in the mid-infrared. Both sources have been suggested to belong to a physical bound binary system of young massive Class I objects and create their own ultra-compact HII regions. The latest deep near-IR survey [11] and the current Chandra X-ray observation introduced many more NEW point sources detected within this area [see Figure [10]]. If the current theory is correct than Chandra detected the variable [see Figure [11 left]] X-ray emission from the high-mass protostellar object IRS 5S, the younger companion of IRS 5 system. Another interesting hard X-ray source (labeled as 6), seen in projection even closer to the IRS 5N than IRS 5S, exhibits even more prominent flare [Figure [11 middle]].

EMBEDDED OBJECT 182022.8-161148

The P3(1R3) sub-millimeter clump, harboring one of the 4 known water masers, lies half arcminutes to the west from M17-UC1 region and is a part of the northern condensation in the M17SW complex [see Figure [9]]. The derived mass and luminosity of the clump are consistent with it being the site of the formation of stars with masses > 10 solar mass [8]. Many authors have noted the association between water masers and the earliest stages of stellar evolution: maser emission may arise as the result of a molecular outflows that occur early in the formation of a massive star in a region of a very dense molecular clump [e.g. 3]. Chandra detected two X-ray sources within the P3 clump [see Figure [12]]. The red source is presumably a flaring T-Tauri star located in front of the clump, JHK colors suggest Class II. The blue source is very hard, has no counterparts, has 22 counts, the median energy of 4.8 keV, and is not variable [see Figure [11 right]]. The projected distance between the water maser and this source is only $1.5''$ (~ 2500 AU). In order to get an estimate of the plasma temperatures we extracted X-ray spectrum and fitted it with a single-temperature "mekal" model plus absorption. As the number of detected photons is rather small, the fitting parameters are necessarily associated with rather larger uncertainties. The fit yields a plasma temperature of $kT \sim 4.4$ keV and a column density of $n_H \sim 1.9 \times 10^{23}$ cm $^{-2}$ ($A_V \sim 95$ mag), while the visual extinction through the center of P3 clump is $A_V \sim 450$ mag [8]. The corrected X-ray luminosity derived from this fit is $\log L_x \sim 31.5$ erg/s [see similar results in [19]]. Did we detect a Class 0 protostar?